

Fabrication of room temperature-stable $12\text{CaO} \cdot 7\text{Al}_2\text{O}_3$ electride: a review

Sung-Wng Kim · Satoru Matsuishi ·
Masashi Miyakawa · Katsuro Hayashi ·
Masahiro Hirano · Hideo Hosono

Published online: 28 March 2007
© Springer Science+Business Media, LLC 2007

Abstract $12\text{CaO} \cdot 7\text{Al}_2\text{O}_3$ (C12A7) electride, which is synthesized by replacing free oxygen ions in cages with electron anions, has distinct advantages over electrides reported so far in respect of thermal and chemical stability and flexible preparation of various sample forms including single crystal, thin film, polycrystalline bulk and powder. These advantages, together with the fact that the concentration of the electron anions is controlled in a wide range according to a synthetic process, make the C12A7 electride attract growing attentions from both scientific and practical points of views. This paper reviews several chemical and physical synthetic processes of the C12A7 electride including thermal treatment of C12A7 under metal vapor and reducing gas atmospheres, hot Ar^+ ion implantation, solidification of the strongly reduced C12A7 melt, and crystallization of the reduced glass in vacuum. Each process, having its own suitability for a specific form of the electride, has unique advantages such as a completeness of anion replacement, mass production capability and controllability of the electron-doped area. Electronic and optical properties of the resulting electrides prepared by the different process are briefly discussed in terms of the feature of the processes.

1 Introduction

Electride [1, 2] is an exotic ionic material in which an electron occupies crystallographic site, acting as an anion. Two major classes of electride, organic and inorganic, have been developed so far. The first electride was synthesized using a combination of an organic molecule and an alkali metal element, where electrons, produced by the ionization of the metals, localize in cavities embedded in the positively charged framework composed of the ionized molecules [1]. The organic electrides are, unfortunately, unstable at room temperature (RT), degrading upon the exposure to air or moisture although the stability is much improved in the recently found $\text{Na}^+(\text{TriPip}222)(\text{e}^-)$ [3]. On the other hand, zeolites heavily doped with alkali atoms form the inorganic electride, where the positively charged alkali atoms construct ordered zigzag chains and their positive charges are compensated by the electron anions localized near the chain [4]. We have developed another type of the inorganic electride, which is far more stable thermally and chemically than the other electrides, using nanoporous crystal C12A7 as a precursor where free oxygen ions in intrinsic cages embedded in the positively charged framework are replaced by the electron anions [5–9]. The C12A7 electride has unique characteristics such that the concentration of the electron anions is systematically controllable in a wide range depending on a preparation condition and various forms of the electride including single crystal, powder and thin film have been prepared by different processes.

The ordered distribution of the electron anions in the electride, which is a novel type of low density electron gas or plasma, is never found in conventional materials such as electron-doped semiconductors [3]. Because of the

S.-W. Kim (✉) · S. Matsuishi · M. Miyakawa ·
K. Hayashi · M. Hirano · H. Hosono
Frontier Collaborative Research Center, Tokyo Institute of
Technology, 4259 Nagatsuta, Midori-ku, Yokohama 226-8503,
Japan
e-mail: sw-kim@lucid.msl.titech.ac.jp

exceptional features of electrides originating from the electron anions, they are attracted much attention from a view point of material science. In addition, since the electrons in electrides are loosely bound to the crystal lattice, they may drift over the crystal lattice upon the external electric field, inducing the electrical conductivity and can be extracted easily from the lattice, causing the electron emission at low temperatures [8, 10–12]. Further, the electrons are possibly transferred to chemical substances through the electride surface, resulting in the reduction of the substances. Such behaviors of the anionic electrons allow for the realization of various novel applications including electrical wiring, electron injection electrode, cold electron emitter, thermionic power generator and reducing agent [1]. For the fundamental research and development for the applications, it is strongly desirable to prepare various forms of the electride. Therefore, the flexibility in the form of the C12A7 electride, especially successful growths of a single crystal and an epitaxial thin film, are much desirable in clarifying intrinsic properties of the electride as well as in realizing versatile applications.

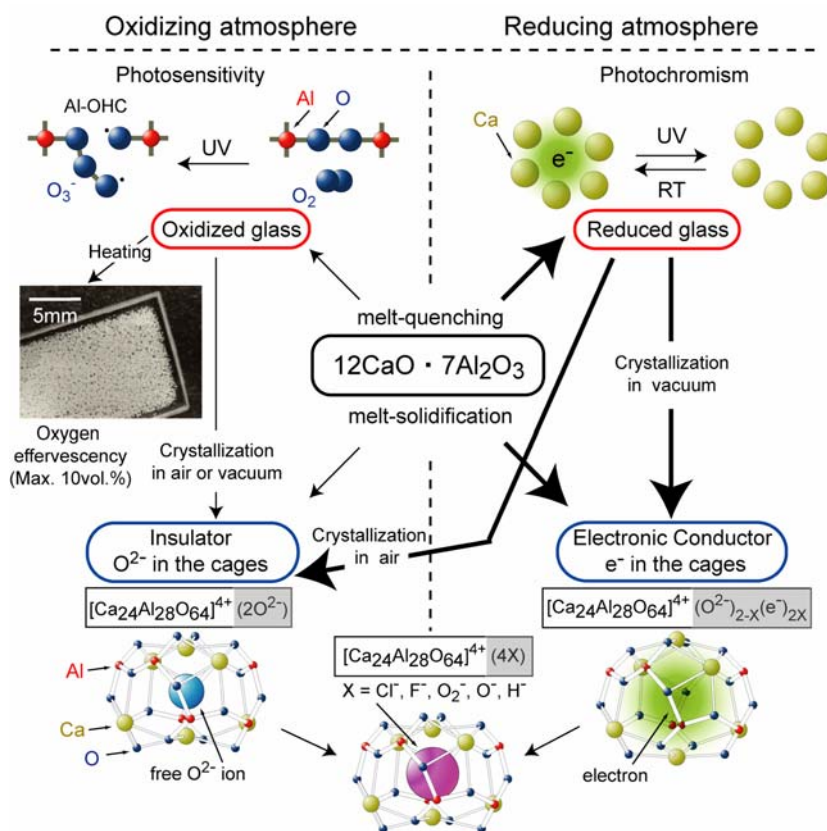
In this paper, we review several synthetic processes that we have developed for the C12A7 electride and briefly refer to optical and electrical properties of various forms of the electride.

2 Synthesis process of C12A7 electride

2.1 Feature of C12A7 and C12A7 electride

C12A7 is a member of CaO–Al₂O₃ mixed oxide compound system [13–16]. However, it exhibits exceptional features from the other compounds of CaO–Al₂O₃ system. For example, C12A7 easily forms a glass and the density (2.69 g·cm⁻³) in the solid phase is smaller than that (2.75 g·cm⁻³) in the liquid phase [17]. Figure 1 represents the characteristics of calcium aluminate glass and crystalline C12A7. It also exhibits fast ion conduction [18, 19], and the fundamental optical absorption edge shifts much lower energy side compared to other CaO–Al₂O₃ compounds [20]. These properties mostly come from a unique crystal structure of C12A7. The unit cell with a stoichiometric composition is composed of two formula of C12A7 and represented as [Ca₂₄Al₂₈O₆₄]⁴⁺(2O²⁻). The former is a positively charged lattice framework that contains 12 sub-nanometer-sized cages with an inner free space of ~0.4 nm in diameter. Thus, each cage has a mean effective charge of +1/3 (+4 charges/12 cages) and it is connected with a neighbor cage by sharing a Ca–O–Al–O–Al–O 6-atom ring. To compensate for the positive charge of the lattice framework, two free O²⁻ ions, which are the

Fig. 1 Characteristics of calcium aluminate glass and crystalline 12CaO · 7Al₂O₃ both in oxidizing and reducing atmospheres



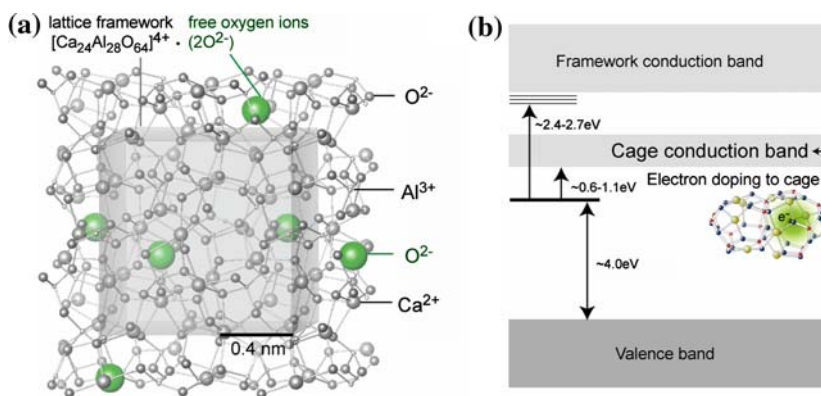


Fig. 2 (a) Crystal structure of $12\text{CaO} \cdot 7\text{Al}_2\text{O}_3$. Structure of the lattice framework viewed along the $\langle 100 \rangle$ direction. Gray frame indicates a cubic unit cell, $[\text{Ca}_{24}\text{Al}_{28}\text{O}_{64}]^{4+}$, with the lattice constant of 1.199 nm. Two free O^{2-} ions are incorporated in two cages out of the twelve to preserve charge neutrality. (b) Schematic of energy levels of the electron incorporated C12A7. The cages are three-dimensionally connected through a monomolecular-thick cage wall

most unique characteristic of this crystal, are located in two different cages in the framework and the other 10 cages are empty (Fig. 2(a)). The free O^{2-} ions can be replaced by various monovalent anions including halogen anions (F^- , Cl^-) [13–16], hydroxide ions (OH^-) [13, 14, 15, 16], superoxide radicals (O_2^-) [21], oxygen anion radicals (O^-) [22, 23], and hydride ions (H^-) [24–26] due to suitable chemical and physical treatments. These active anions exhibit exceptional functions such as strong oxidative ion beam emission (O^-) [23] and persistent photo-induced insulator-conductor conversion (H^-) [24–26]. Furthermore, they are almost exclusively replaced by electrons [5]. Thus, the replacement of two free oxygen ions by four electrons leads to the formation of $[\text{Ca}_{24}\text{Al}_{28}\text{O}_{64}]^{4+}(4\text{e}^-)$, which is regarded as a new type of inorganic electride because the trapped electrons are semi-localized at the cage sites acting as anions. In this paper, C12A7 containing the electron anions is referred to as “C12A7 electride” or “C12A7: e^- ”, although electride is defined by $[\text{Ca}_{24}\text{Al}_{28}\text{O}_{64}]^{4+}(4\text{e}^-)$ in the strict definition.

2.2 Synthetic process of C12A7 electride

Once the C12A7 framework is formed, the encaged free oxygen ions can be replaced by the electrons maintaining the framework when the stoichiometric C12A7 is exposed to a reducing environment. Practical reducing atmospheres have been achieved by metal vapor (process 1) [6] and reducing gas such as CO/CO_2 (process 2) [9]. In addition to these “chemical processes”, a novel physical process of hot Ar^+ ion implantation in C12A7 films (process 3) [6] have been developed. These chemical and physical processes inevitably require a specific form of C12A7 as a

precursor for the electride formation. The precursors include single crystals grown by a floating zone (FZ) [27] and Czochralski (CZ) [28] techniques, powder and thin film. In addition to these two-step processes, we have developed a simple process where the electride is directly synthesized through the solidification from C12A7 melt (process 4) [7, 8] and the crystallization of an oxygen deficient glass (process 5) [7, 8]. Table 1 summarizes the precursors, reaction processes and electride quality in terms of electron concentration of each process.

Each process has inherent advantages and suitability for specific forms of C12A7. For instance, the free oxygen ions are almost exclusively replaced by electrons in process (1), making it possible to prepare the single crystal electride, while processes (4) and (5) are well-suited for a mass production of polycrystalline electride, and process (3) is a clean physical process suited for the preparation of thin film electride.

and large free space in the C12A7 cages forms an additional conduction band named “cage conduction band”. The electrons entrapped in the cages migrate through the cages, leading to the electronic conduction. The lower energy excitation (0.6–1.1 eV) is due to inter-cage charge transfer transition and the higher energy one (2.4–2.7 eV) corresponds to intra-cage transition. The latter transition is responsible for the coloration

2.2.1 Thermal treatment in metal vapor atmosphere

Some of metals deposited on the surface of C12A7 react with the free oxygen ions at the surface to form metal oxides. Such reaction leads to the extraction of the free oxygen ions from the cages and trapping of the electrons in the cages. The replacement of the entrapped species may proceed from surface to inside of bulk with an aid of the oxide ion diffusion at high temperatures. Thus, the process results in the reduction of C12A7 to form the electride, indicating the metal vapor acts as a reducing atmosphere for the stoichiometric C12A7. Ca metal vapor has been employed initially although we have quite recently found Ti metal is superior to Ca metal in terms of exclusive

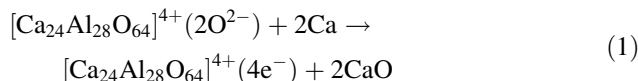
Table 1 Summary of C12A7 electrified preparation processes

Process		Precursor	Reacting Process	N_{F+} (cm ³)
Chemical process	Ca vapor treatment	Single crystal	$C12A7:O^{2-} + 2Ca \rightarrow C12A7:e^- + 2CaO$	$\sim 10^{21}$
	Ti vapor treatment	Single crystal/Powder	$C12A7:O^{2-} + Ti \rightarrow C12A7:e^- + TiO_x$	$\sim 10^{21}$
	Melt-solidification	No specific one	$C_2^{2-}(\text{melt}) \rightarrow C12A7:C_2^{2-}$ $\rightarrow C12A7:e^- + 2C$ or $C_2^{2-} + O^{2-} \rightarrow C12A7:e^- + 2CO$	$\sim 10^{19}$
	Glass-ceramics	No specific one	$C_2^{2-}(\text{glass}) \rightarrow C12A7:e^- + 2C$ or $C_2^{2-} + O^{2-} \rightarrow C12A7:e^- + 2CO$	$\sim 10^{19}$
	Reducing treatment in CO gas	Single crystal/Powder	$C12A7:O^{2-} + CO \rightarrow C12A7:e^- + CO_2$	$\sim 10^{20}$
Physical process	Ion implantation	Thin film	$C12A7:O^{2-} \rightarrow C12A7:e^- + 1/2O_2$	$\sim 10^{21}$
			or $C12A7:OH^- \rightarrow C12A7:H^- + 1/2O_2$ $\xrightarrow{UV} C12A7:e^- + H_2$	

replacement of the free oxygen ions and short process duration.

C12A7 single crystals are sealed in a silica glass tube (inner volume ~ 10 cm³) with Ca metal shots under a vacuum of $\sim 10^{-3}$ torr (Ca-treatment). Then, the sealed tube is heated at 700 °C for 4–240 h (Fig. 3). With an increase in the Ca treatment duration, the sample color changes from colorless transparent to green, and finally it becomes black (Fig. 2). X-ray diffraction pattern reveals that the sample surfaces are covered with a crystalline CaO layer after the reaction was completed. The formation of CaO layer is attributed to the reaction between the free oxygen ions in the crystal and the Ca metal deposited on the sample surface. Because a C12A7 crystal shows the high oxygen ion conduction, the free oxygen ions in the cages diffuse to the surface and react with Ca metal to form a CaO layer at high temperatures. During the extraction

process of free oxygen ions, the electrons are incorporated in the cages to maintain the charge neutrality (Fig. 4). These facts indicate that the Ca treatment does not destroy the lattice framework of C12A7, but only induces the replacement of the free oxygen ions by electrons. Thus, the formation mechanism for the C12A7 electrified is expressed as follows:



2.2.2 Thermal treatment in reducing gas atmosphere

The reduction for C12A7 is also achieved when C12A7 is exposed to reducing gas atmosphere. Hydrogen molecules, which may produce strong reduction atmosphere, are not used for the electrified formation because H⁻ ions are incorporated in the cages when C12A7 is thermally treated in atmosphere containing hydrogen. Thus, we have employed a mixture of CO and CO₂ gas, in which partial oxygen pressure (PO_2) is below 10^{-15} atm. A pellet of C12A7 powder, placed in a carbon crucible with a cap, is heated at 1000–1200 °C for ~ 24 h in a flowing N₂ gas atmosphere (Fig. 5). The atmosphere inside the carbon crucible during the treatment is likely strongly reductive CO/CO₂ with $PO_2 = 10^{-19} \sim 10^{-17}$ atm.

Because of the strongly reductive atmosphere, oxygen vacancies are formed at the cage sites by CO gas reacting with the free oxygen ions to form CO₂ gas. To compensate for the positive charge of the lattice framework, electrons are injected into the cages instead of the extracted free oxygen ions. The treatment changes the sample color to green due to the induction of an absorption band at 2.8 eV. It also enhances the electrical conductivity up to ~ 4 S · cm⁻¹ at 300 K. These observations indicate that the

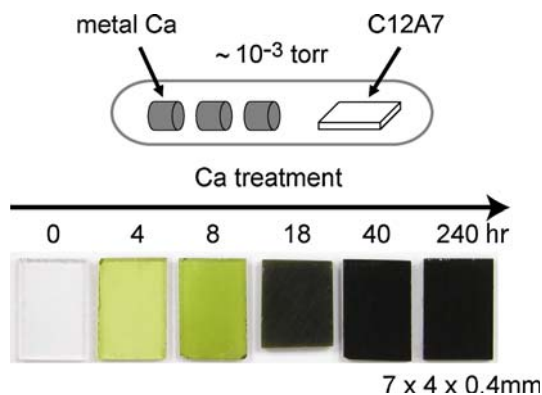


Fig. 3 Schematic illustration of the synthesis process for C12A7 electrified via Ca treatment. FZ grown C12A7 single crystal was sealed in a silica glass tube with Ca metal shots under a vacuum of $\sim 10^{-3}$ torr and heated at 700 °C for 4–240 h. The Ca treatment changes the sample color from colorless to green, and finally to black, with increasing duration of the Ca treatment

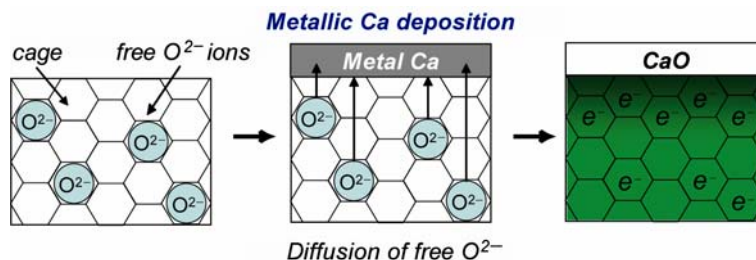


Fig. 4 Formation mechanism for C12A7 electride via Ca treatment. The free oxygen ions in cages are diffused to the surface and react with Ca metal deposited on the sample surface to form a CaO layer at

high temperatures. During the process, the electrons are incorporated in the cages to maintain the charge neutrality with lattice framework

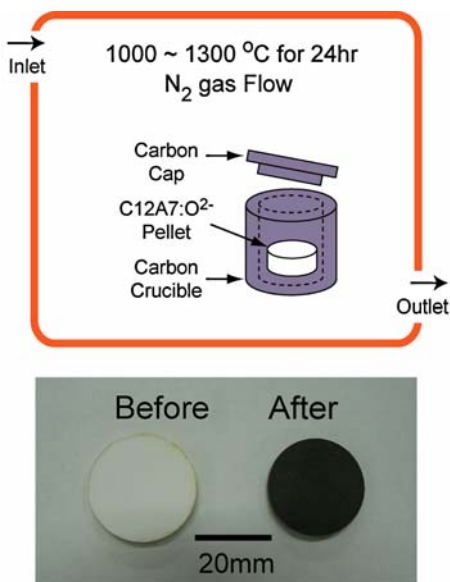
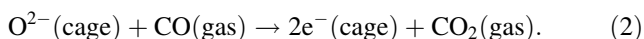


Fig. 5 Schematic illustration of synthesis process for C12A7 electride via reduction treatment and photograph of obtained dark green electride pellet (φ 25 mm \times 2 mm). A reducing atmosphere is achieved by heating a carbon crucible with a carbon cap at 1000–1200 °C for ~24 h in a flowing N₂ atmosphere, which corresponds to $P_{O_2} = 10^{-19} \sim 10^{-17}$ atm

electron anions with concentration of $\sim 8 \times 10^{19} \text{ cm}^{-3}$ are incorporated in C12A7 through the thermal treatment in the CO/CO₂ atmosphere. Therefore, the reduction process is described by the following reaction:



This method is applicable to all forms of C12A7 precursors, including single crystal, powder and thin film. Further, unlike the metal vapor treatment which inevitably produces the metal oxide layer at the surface, the sample surface is kept clean without forming any additional products during the reaction. This advantage facilitated the thermodynamic analysis for the C12A7 electride formation [9].

2.2.3 Hot Ar⁺ ion implantation

Ion implantation, one of non-equilibrium physical processes, has several advantages over conventional chemical doping processes such that high concentration of ions can be introduced in a designated small area with an excellent controllability [29, 30], and thus it is widely used for the modification of thin films.

We have conducted Ar⁺ ion implantation into polycrystalline C12A7 thin films and found that the electron anions are incorporated into the cages as a result of kicking out the free oxygen ions from the cages through the nuclear collisions. The polycrystalline C12A7 thin films (~800 nm in thickness) were prepared on MgO(100) single crystal substrates by a pulsed laser deposition technique at RT and a subsequent annealing at 1100 °C for 1 h in air to crystallize the deposited amorphous films. Ion implantation was carried out at temperatures from RT to 600 °C in a vacuum less than $\sim 2 \times 10^{-8}$ torr. The Ar⁺ fluence (accumulated dose) set to vary from 1×10^{16} to $1 \times 10^{18} \text{ cm}^{-2}$. Moreover, the C12A7 framework is stable for the hot implantation, although a crystalline film is converted to amorphous phase if the implantation is performed at RT.

Figure 6 shows the electrical conductivities of Ar⁺-implanted films subjected to the implantation at high temperature of 600 °C as a function of Ar⁺-ion fluence. The electrical conductivity of the film increases with implanted fluence: films with fluences less than $1 \times 10^{17} \text{ cm}^{-2}$ are insulators, while those with $5 \times 10^{17} \sim 1 \times 10^{18} \text{ cm}^{-2}$ exhibit the electrical conductivity of ~ 0.5 and $1 \text{ S} \cdot \text{cm}^{-1}$, respectively. The enhancement of the electrical conductivity is accompanied by the appearance of optical absorption bands at 0.4 and 2.8 eV, indicating the F⁺-like centers are simultaneously formed by the hot implantation. These results suggest that the free oxygen ions are kicked out from the cages by the collision between the free oxygen ions and Ar⁺ ions, leaving electrons in the cages. As a result, the electrons are directly produced by Ar⁺-implantation via the extrusion of free oxygen ions through the following reaction.

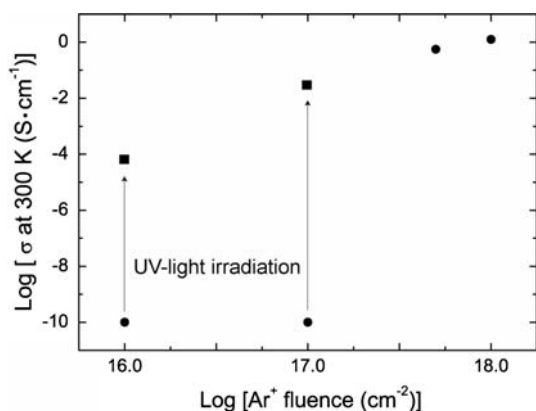
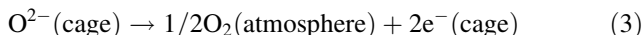
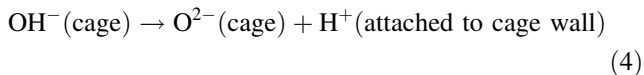


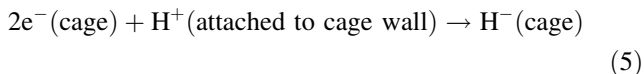
Fig. 6 Electrical conductivity as a function of Ar^+ fluence. Black circle and square represent the electrical conductivities at 300 K of as-implanted and UV-light irradiated thin films after implantation. As-implanted films with a fluence below $1 \times 10^{17} \text{ cm}^{-2}$ were insulators. A subsequent UV-light irradiation on as-implanted films with a fluence below $1 \times 10^{17} \text{ cm}^{-2}$ also exhibited the electronic conduction



It is noted in lower fluence samples $<1 \times 10^{17} \text{ cm}^{-2}$ that the conductivity and the optical absorption intensities increase after UV light irradiation. Since these phenomena are commonly observed in H^- incorporated C12A7, it suggests that H^- ions are introduced into the cages by the hot implantation of Ar^+ ions. We consider that the formation of the H^- ions by Ar^+ -implantation is caused by pre-existing OH^- groups that might be introduced during post-annealing process for the crystallization of amorphous films in air. That is, electrons are generated by the extrusion of free oxygen ions through the reaction (3) and simultaneously protons (H^+) are created by the decomposition of pre-existing OH^- groups in the as-prepared film through the reaction (4).



Then, H^+ ions immediately react with the electrons in the cages, leading to the formation of H^- ions (reaction 5).



Thus, H^- ions are formed in lower fluence samples by hot implantation of Ar^+ ions, leading to the light-induced electronic conduction and coloration.

Figure 7 shows the schematic illustration of the electron and H^- formations by Ar^+ -implantation as mentioned above. Ar^+ -implantation produces the electrons and protons in the cages by nuclear collisions and electronic excitation

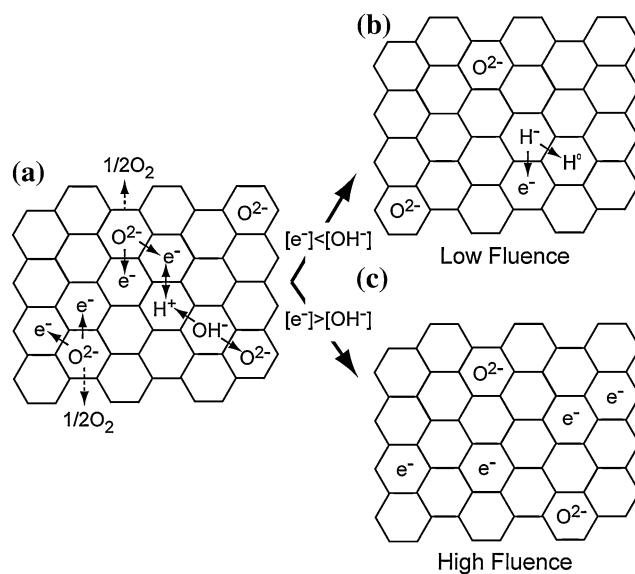


Fig. 7 Model for the formation of electrons and hydride ions in cages by hot inert ion implantation. The hexagonal represents a crystallographic cage of C12A7. (a) The formation of electrons and protons during the implantation and (b, c) The incorporated anions in the cages after the implantation with low and high fluences

effects through the reactions (3) and (4). When the number of the electrons produced by reaction (3) is less than that of protons (Fig. 6(a)), all of produced electrons are captured by H^+ ions through reaction (5) (Fig. 6(b)) and H^- ions are formed in the cages. However, when the generated electron concentration exceeds the proton concentration, the excess electrons themselves are directly introduced into the cages (Fig. 6(c)).

Since higher concentration of the electrons are incorporated three-dimensionally in a designated narrow space, the synthesis of the C12A7 electride thin films by the ion implantation paves a way to realize novel applications such as patterned electric wiring, electron injection electrode and cold electron emitter.

2.2.4 Direct synthesis of C12A7 electride from melt and glass states

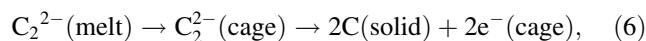
Melt-solidification and glass-ceramics process. The development of a simple synthesis process, which is compatible for mass production of the electride, is strongly required for practical applications. Possible candidate to satisfy the requirement is a direct synthesis of the electride from the melt or glass state. Extensive studies regarding the relationship between melting condition and corresponding precipitated phases in $\text{CaO-Al}_2\text{O}_3$ system [16, 17] verify that the presence of template anions to compensate the positive charge of the C12A7 framework is inevitable for the precipitation of the C12A7 phase. More specifically, the C12A7 phase is reproducibly prepared from the

stoichiometric C12A7 melt in wet air [16], involving O^{2-} and/or OH^- ions that act as the template. On the contrary, the thermal treatment in inert gas atmospheres, where template anions are seemingly absent, hinders the formation of the C12A7 phase and only a mixture phase of C3A ($3CaO \cdot Al_2O_3$) and CA ($CaO \cdot Al_2O_3$) is formed. If we could precipitate the crystalline C12A7 under an appropriate reducing atmosphere, there is a possibility to synthesize the C12A7 electride directly from the melt or glass phase. Thus, a critical issue for the direct synthesis is to find a novel template ion that can exist in the melt or glass phase even when they are exposed to reducing atmospheres. With efforts in searching for such templates, we have successfully prepared the C12A7 electride directly from the melt or glass state where C_2^{2-} ion most likely acts as a template for the C12A7 phase formation.

Figure 8(a) shows schematically a direct solidification process to prepare the electride from the C12A7 melt. C12A7 powders of the stoichiometric mixture of CaO and Al_2O_3 are melted in a semi-airtight carbon crucible with a carbon cap at 1600 °C for 1 h in air. Heating the carbon crucible at 1600 °C produces a strongly reducing atmosphere ($PO_2 = \sim 10^{-16}$ atm) inside the crucible. The crucible is slowly cooled down at a rate of ~ 400 °C · h⁻¹. X-ray diffraction measurements clarify that solidified products are mixtures of C3A and CA. Then, they are re-melted and solidified again according to the same temperature profile as that of the first run. The second run results in the formation of the C12A7 crystalline phase with a green color and the electrical conduction.

Raman spectra of the products after the first run and thermal desorption measurement in the cooling process in

the second run suggest that C_2^{2-} ions are dissolved into the melt from the carbon crucible to compensate for the oxygen deficiency caused by the strongly reducing atmosphere. Furthermore, the ionic radius of C_2^{2-} (1.2 Å) is similar to O^{2-} (1.4 Å), which supports that the C_2^{2-} anions serve as the template in a reducing atmosphere, instead of the free oxygen ions in an oxidizing atmosphere. Moreover, the C_2^{2-} Raman band is not observed in the electride and CO gas is evolved in the cooling process, which implies that the encaged C_2^{2-} ions are only stable in the nucleation and/or initial stage of the crystallization and they are released from the cages, leaving electrons in the lattice during the cooling process. Thus, the electron formation processes in the cages may be expressed as follows:



and/or

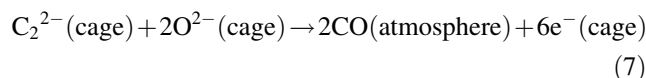


Figure 8(b) shows schematically the glass-ceramics process for the preparation of the electride. Oxygen deficient glass, which is obtained by a rapid quench of the C12A7 melt in a carbon crucible placed in air, is crystallized in an evacuated silica tube by heating to 1000 °C, which is higher than the crystallization temperature (> 900 °C). The resultant C12A7 samples were green in color and exhibited rather high electrical conductivity, indicating that electrons are incorporated into the cages instead of free oxygen ions. Similar to the direct

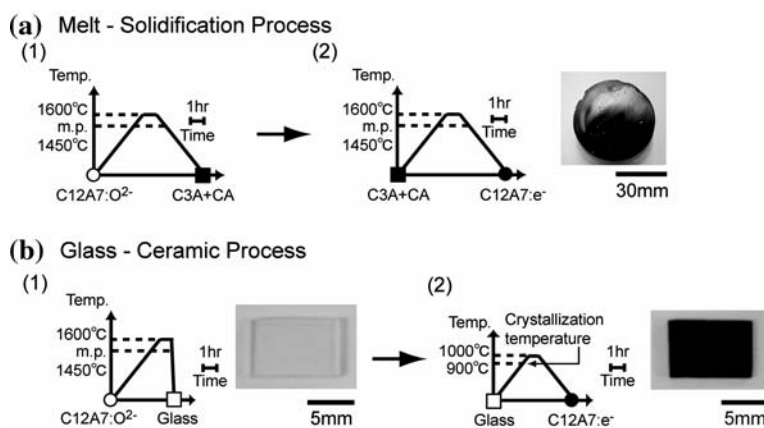


Fig. 8 Schematic illustration of synthesis processes for C12A7:e⁻ via melt. **(a)** Melt-Solidification Process. Temperature profiles for the electride formation by the solidification of the reduced C12A7 melt and a photograph of the obtained dark green electride ($\varphi 50$ mm × 10 mm) are shown. The reducing atmosphere is achieved by heating a carbon crucible with a carbon cap at 1600 °C in air. **(b)** Glass-ceramics process. The transparent reduced glass is obtained by

quenching the melt according to the temperature profile (1). The glass is encapsulated in a SiO₂ glass ampoule under a vacuum and heated at 1000 °C for 30 min. Photographs of the reduced glass and the obtained C12A7:e⁻ show that the crystallization converts the transparent reduced glass into polycrystalline electride exhibiting dark green color

melt-solidification process, C_2^{2-} ions, which are likely incorporated in the glass, are considered to act as the template.

3 Optical and electronic properties of C12A7 electride

3.1 Electronic structure and properties

The empty cages in the C12A7 framework form an additional conduction band named ‘‘cage conduction band (CCB)’’ [31, 32], which is split from the framework conduction band (FCB) and locating ~ 2 eV below FCB minimum (Fig. 2b). In stoichiometric C12A7, where two free oxygen ions occupy different cages, $2p$ electrons of the oxide ions form localized levels which are located far below CCB. Thus, the stoichiometric C12A7 is a band insulator. When a small number of electrons are introduced into CCB due to the replacement of a portion of the free oxygen ions by electrons, the electron is localized in a cage due to a large distortion of the cage geometry creating an F^+ -like center or the electron forms ‘‘polaron’’ [31]. Thus, C12A7 containing a small number of electrons exhibits semiconductor type electrical conduction because the electron can move by hopping among cages with an assistance of thermal energy [6]. With an increase in electron concentration, the cage distortion becomes smaller, which enhances the delocalization of the electron and finally the C12A7 electride, where four electrons occupy CCB, exhibits metallic conduction. Thus, the electrical conductivity increases with the electron concentration and accordingly the conduction type changes from insulator to semiconductor and finally to metallic. In other words, the electrical conductivity provides a qualitative measure for the electron concentration in C12A7.

Figure 9(a) shows the temperature dependence of the electrical conductivity for the Ca-treated single crystals.

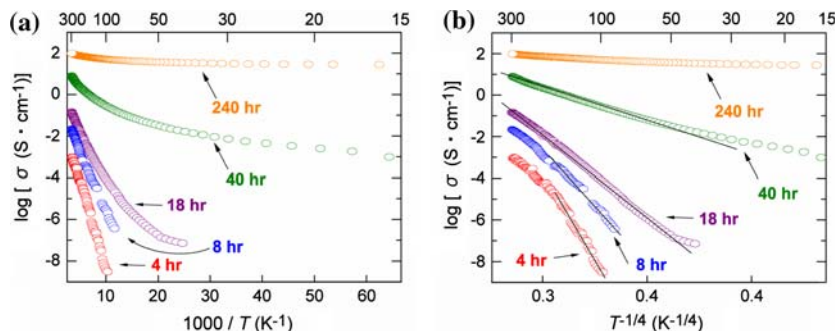


Fig. 9 Temperature dependence of electrical conductivity for Ca-treated C12A7 single crystals. The electrical conductivity was measured using a conventional four-probe method in a temperature range from RT to 2 K, employing sputtered Pt film as electrodes. (a) $\log \sigma$ versus T^{-1} plot. (b) $\log \sigma$ versus $T^{-1/4}$ plot. For Ca-treated

The Ca treatment at 600 °C for 4 h leads to a drastic enhancement of the conductivity to $10^{-3} \text{ S} \cdot \text{cm}^{-1}$ from that of as-grown crystals whose conductivity is lower than that of detectable limit of $10^{-10} \text{ S} \cdot \text{cm}^{-1}$. It further increases with the increase in the Ca treatment duration and reached to $\sim 100 \text{ S} \cdot \text{cm}^{-1}$ for the Ca treatment for 10 days. The intensity of 2.8 eV band reveals the electron concentration is $\sim 2 \times 10^{21} \text{ cm}^{-3}$. The logarithm of the electrical conductivity is proportional to $T^{-1/4}$ and not T^{-1} over a wide temperature range of 300–50 K (Fig. 9(b)), suggesting that the electron can move through the crystal by hopping [6].

Figure 10(a) shows the temperature dependence of the electrical conductivity for the polycrystalline C12A7:e⁻ prepared by the melt-solidification process. The conductivities at 300 K for the C12A7:e⁻ by the melt-solidification and the glass-ceramics processes are 5 and 1 $\text{S} \cdot \text{cm}^{-1}$, respectively, both exhibiting the semiconductor type. Figure 10(b) shows the correlation between the electrical conductivity and the concentration of the electron anion for the melt-solidified polycrystalline C12A7 and the Ca vapor treated single crystal. The data on $\log \sigma$ and $\log N_{F^+}$ for the polycrystalline electride are close to those of the single crystal electride, indicating that the carrier mobilities ($\sim 0.1 \text{ cm}^2 \cdot \text{V}^{-1} \cdot \text{s}^{-1}$) are nearly the same between two samples. This agreement suggests the polycrystalline sample is composed of tightly connected large grains ($\sim 3 \text{ mm}$)[7], which may largely reduce a deteriorative grain boundary effect on the electronic transport.

3.2 Optical properties

Two optical absorption bands peaking at 0.4 and 2.8 eV are induced due to the incorporation of the electron anions as shown in Fig. 11. The latter band is responsible for the green coloration of the C12A7 electride. Ab initio calculations for the C12A7 electronic structure verify that the

samples for 18 and 40 h, $\log \sigma$ is proportional not to T^{-1} but to $T^{-1/4}$ over a whole temperature range, 300–50 K. This characteristic implies that the conduction is controlled by a variable range hopping. For the most highly conductive sample, $\log \sigma$ is almost constant in the temperature region

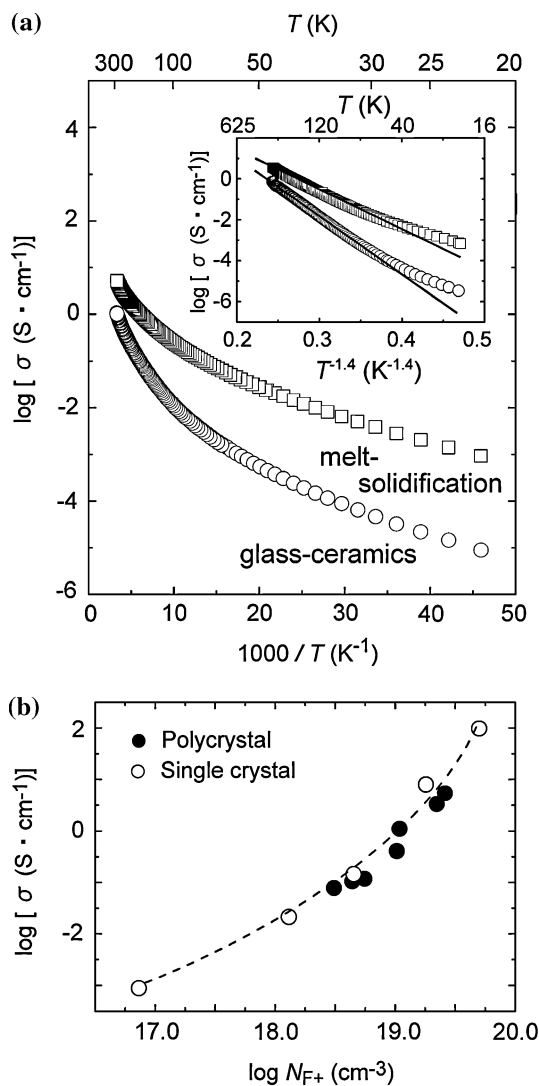


Fig. 10 (a) Temperature dependence of electrical conductivity for C12A7:e⁻ prepared by melt-solidification and glass-ceramics processes. The electrical conductivity was measured using the four-probe method in a temperature range from RT to 2 K, employing sputtered Pt film as electrodes. Inset shows log σ as a function of $T^{-1.4}$. (b) Electrical conductivity (σ) versus F^+ -like center concentration (N_{F^+}) as determined by EPR at 300 K for polycrystalline (black circle) and single crystal electrides (open circle). It is evident that the electron mobility of the polycrystalline electrides obtained via the melt is similar to that of single crystal electride

absorption band at 0.4 eV is due to an inter-cage *s*-to-*s* transition (from an electron-trapped cage to a vacant neighboring cage), while that at 2.8 eV is attributed to an intra-cage *s*-to-*p* transition of the trapped electrons in the cages [32]. The intensity of the 2.8 eV band increases proportional to the concentration of the electrons in the cages. On the other hand, the 0.4 eV band exhibits a saturation behavior because the number of the empty cages decreases with an increase in the electron concentration. This indicates that the concentration of the electron is

evaluated precisely by the intensity of the 2.8 eV band. Using this evaluation technique, the electron concentration in the Ca vapor treated electrides are evaluated to be $1 \times 10^{19} \sim 2 \times 10^{21}$, while those in C12A7 prepared by the glass-ceramics and melt-solidification processes are estimated to be $1 \times 10^{19} \sim 3 \times 10^{19} \text{ cm}^{-3}$.

The electron anion is also detected by electron spin resonance (ESR) spectroscopy. The C12A7 electride with low electron concentration ($\sim 10^{19} \text{ cm}^{-3}$) shows an EPR signal with an isotropic shape that appears at $g = 1.994$ (Fig. 12). The signal is assigned to the F^+ -like center where an unpaired electron is trapped at the site coordinated by six Ca^{2+} ions attached to the cage wall [24]. However, the intensity tends to saturate in a high electron concentration region ($> \sim 10^{19} \text{ cm}^{-3}$) presumably due to the formation of pairs where the electron spins are coupled anti-parallel [6].

4 Summary

A variety of the chemical and physical preparation processes for the C12A7 electride are reviewed. The characteristic features of each process are summarized as follows.

- (1) The single crystal electride is synthesized by the thermal treatment of C12A7 under active metal (Ca, Ti) vapor atmosphere in which metal oxides are formed at sample surface through the reaction of deposited metals and free oxygen ions. This process is the most efficient to synthesize the single crystal electride with a high electron concentration of $\sim 2 \times 10^{21} \text{ cm}^{-3}$.
- (2) The thermal treatment under reducing gas (CO/CO_2) atmosphere makes possible to synthesize all forms of C12A7 electride via the reduction of free oxygen ions. This process does not produce any additional products, which makes the process more favorable to synthesize the powder electride than other processes.
- (3) The C12A7 thin film electride is prepared by the hot Ar^+ ion implantation process, in which the free oxygen ions are extracted by kicking out effect through the nuclear collisions. The process provides the stable synthesis of thin film electride although a crystalline film is converted to amorphous phase if the implantation is performed at RT. It also provides advantages inherent to physical process, i.e. the possibility in controlling the electron concentration precisely.
- (4) Bulk polycrystalline electrides are directly synthesized without specific forms of C12A7 precursors from the reduced C12A7 melt and glass state, i.e. a solidification of the reduced melt and a crystallization of the reduced glass. These processes are suitable for the mass production of the C12A7 electride.

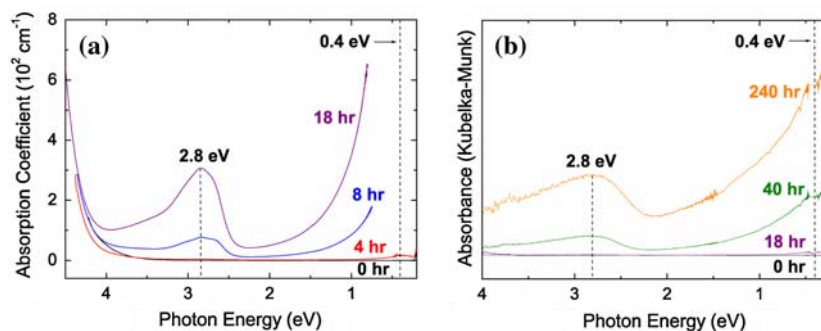


Fig. 11 (a) Optical absorption spectra of as-grown C12A7 and Ca-treated C12A7 single crystals. The Ca treatment induces absorption bands peaking at 2.8 and 0.4 eV. With an increase in the Ca treatment duration, the peak intensities increase. (b) Diffuse reflectance spectra

of Ca-treated samples. The samples were crushed into fine powders and diluted with KBr powder for the measurements. The absorption spectra were obtained by Kubelka-Munk transformation

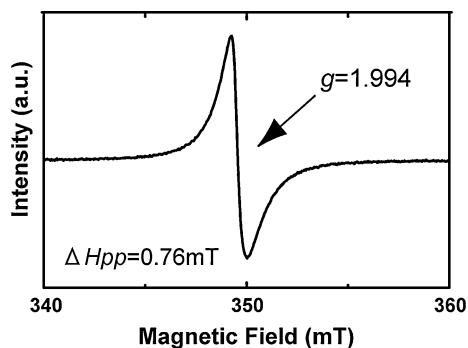


Fig. 12 X-band EPR spectrum of polycrystalline C12A7:e⁻ with electron concentration of $\sim 3 \times 10^{19} \text{ cm}^{-3}$ prepared by melt-solidification process. The carrier electron concentration was determined by electron paramagnetic spin resonance (EPR) using a Bruker E580 X-band (~ 9.7 GHz) spectrometer at RT. To avoid the skin depth effect due to carrier electrons, the samples were crushed into fine powders ($\sim 1 \mu\text{m}$ in diameter). The spin concentration was estimated by comparing the second integral of the spectrum with that of $\text{CuSO}_4 \cdot 5\text{H}_2\text{O}$ standard

Acknowledgements This work was supported by a Grant-in-Aid for Creative Scientific Research (No. 16GS0205) from the Japanese Ministry of Education, Culture, Sports, Science and Technology

References

- J.L. Dye, *Inorg. Chem.* **36**, 3816 (1997)
- J.L. Dye, *Science* **301**, 607 (2003)
- M.Y. Redko, J.E. Jackson, R.H. Huang, J.L. Dye, *J. Am. Chem. Soc.* **127**, 12416 (2005)
- A.S. Ichimura, J.L. Dye, M.A. Cambor, L.A. Villaescisa, *J. Am. Chem. Soc.* **124**, 1170 (2005)
- S. Matsuishi, Y. Toda, M. Miyakawa, K. Hayashi, T. Kamiya, M. Hirano, I. Tanaka, H. Hosono, *Science* **301**, 626 (2003)
- M. Miyakawa, Y. Toda, K. Hayashi, M. Hirano, T. Kamiya, N. Matsunami, H. Hosono, *J. Appl. Phys.* **97**, 023510 (2005)
- S.W. Kim, M. Miyakawa, K. Hayashi, T. Sakai, M. Hirano, H. Hosono, *J. Am. Chem. Soc.* **127**, 1370 (2005)
- S.W. Kim, Y. Toda, K. Hayashi, M. Hirano, H. Hosono, *Chem. Mater.* **18**, 1938 (2006)

- S.W. Kim, K. Hayashi, I. Tanaka, M. Hirano, H. Hosono, *J. Am. Ceram. Soc.* **89**, 3294 (2006)
- Y. Toda, S. Matsuishi, K. Hayashi, K. Ueda, T. Kamiya, M. Hirano, H. Hosono, *Adv. Mater.* **16**, 685 (2004)
- R.H. Huang, J.L. Dye, *Chem. Phys. Lett.* **166**, 133 (1990)
- Y. Toda, S.W. Kim, K. Hayashi, M. Hirano, T. Kamiya, H. Hosono, T. Haraguchi, H. Yasuda, *Appl. Phys. Lett.* **87**, 254103 (2005)
- H.B. Bartl, T. Scheller, *N. Jb. Miner. Mh.* **35**, 547 (1970)
- J. Jeevaratnam, F.P. Glasser, L. S.D. Glasser, *J. Am. Ceram. Soc.* **47**, 105 (1964)
- J.A. Imlach, L.S.D. Glasser, P.F. Glasser, *Cement Conc. Res.* **1**, 57 (1971)
- R.W. Nurse, J.H. Welch, A.J. Majumdar, *Trans. Br. Ceram. Soc.* **64**, 323 (1965)
- G.I. Zhmoidin, A.K. Chatterjee, *Cement Conc. Res.* **15**, 442 (1985)
- M. Lacerda, J.T.S. Irvine, F.P. Glasser, A.R. West, *Nature.* **332**, 525 (1988)
- M. Lacerda, A.R. West, J.T.S. Irvine, *Solid-State Ionics* **59**, 257 (1993)
- K. Hayashi, P.V. Sushko, D.M. Ramo, A.L. Shluger, S. Watauchi, I. Tanaka, S. Matsuishi, M. Hirano, H. Hosono, *J. Phys. Chem. B.* **111**, 1946 (2007)
- H. Hosono, Y. Abe, *Inorg. Chem.* **26**, 1192 (1987)
- K. Hayashi, M. Hirano, S. Matsuishi, H. Hosono, *J. Am. Chem. Soc.* **124**, 738 (2002)
- Q. X. Li, K. Hayashi, M. Nishioka, H. Kashiwagi, M. Hirano, Y. Torimoto, H. Hosono, M. Sadakata, *Appl. Phys. Lett.* **80**, 4259 (2002)
- K. Hayashi, S. Matsuishi, T. Kamiya, M. Hirano, and H. Hosono, *Nature* **419**, 462 (2002)
- S. Matsuishi, K. Hayashi, M. Hirano, H. Hosono, *J. Am. Chem. Soc.* **127**, 12454 (2005)
- M. Miyakawa, K. Hayashi, M. Hirano, Y. Toda, T. Kamiya, H. Hosono, *Adv. Mater.* **15**, 1100 (2003)
- S. Watauchi, I. Tanaka, K. Hayashi, M. Hirano, H. Hosono, *J. Cryst. Growth* **237–239**, 801 (2002)
- K. Kurashige et al., *Cryst. Growth & Design* **6**, 1602 (2006)
- J.S. Williams, J.M. Poate, *Ion Implantation and Beam Process* (Academic, New York, 1984)
- P.D. Townsend, P.J. Chandler, and L. Zhang, *Optical Effects of Ion Implantation* (Cambridge University Press, Cambridge, 1994)
- P. Sushko, K. Shluger, K. Hayashi, M. Hirano, and H. Hosono, *Phys. Rev. Lett.* **91**, 126401 (2003)
- P. Sushko, K. Shluger, K. Hayashi, M. Hirano, and H. Hosono, *Thin solid films* **445**, 161 (2003)